Solute Transport in Open-Channel Flows with Submerged Vegetation

Hyeongsik Kang[1], Sung-Uk Choi[2], and Byungwoong Choi[3]

[1]Post Doctoral Research Fellow, Korea Institute of Construction Technology, 2311, Daehwa-dong, Ilsan-gu, Goyang-si, Gyeonggi-do; email: kanghs@kict.re.kr
[2]Professsor, Primary author, School of Civil and Environmental Engineering, Yonsei University, 134 Seodaemun-gu, Shinchon-dong, Seoul, Korea; Tel.: +82-2-2123-2797; Fax.:+82-364-5300; email: schoi@yonsei.ac.kr
[3]Ph.D. Student, School of Civil and Environmental Engineering, Yonsei University; email: bw628@yonsei.ac.kr

ABSTRACT
This paper investigates numerically the characteristics of the solute transport in the open-channel flow with submerged vegetation. The algebraic scalar flux model and the Reynolds stress model are used for the solute transport and flow computations, respectively. The model is applied to a laboratory experiment, showing that the model predicts the mean flow and secondary currents correctly. To study the impact of vegetation on the solute transport, solute transports in the flow with and without vegetation are compared. It is found for vegetated flow that the diffusion process is enhanced near the vegetation height and the resulting turbulent Schmidt number is less than unity.

Keywords: solute transport, algebraic scalar flux model, submerged vegetation, secondary currents

INTRODUCTION
Vegetation is a key element in the aquatic ecosystem. This comes from the environmental roles of the stream, namely improving water quality, providing habitats for macrofauna, and creating amenity for the people. Regarding water quality issue, it has never been explain clearly how vegetation affects solute or sediment transport.

Recent studies have revealed the mean flow and turbulent structures of the open-channel flow with submerged vegetation (Ikeda & Kanazawa, 1996; Ackerman & Okubo, 1993; Choi & Kang, 2004; Shimizu & Tsujimoto, 1994; Lopez & Garcia, 2001 Ghisalberti & Nepf, 2002; Nezu & Onitsuka, 2001; Xiaohui & Li, 2002). However, the vegetation impact on the transport of pollutants or sediment in the flow with submerged vegetation has rarely been studied.

The purpose of this study is to investigate the characteristics of solute transport in the open-channel flows with submerged vegetation. For this, numerical experiments are carried out. The algebraic scalar flux model for the solute transport is used with the Reynolds stress model for the flow. In order to verify the impact of vegetation on the solute transport, solute transport cases in the

33rd IAHR Congress: Water Engineering for a Sustainable Environment

ISBN: 978-94-90365-01-1

flow with and without vegetation are considered. In the comparisons, the discharges per unit width of the two flows are the same, resulting similar Reynolds numbers. The width-to-depth ratios of the cases are kept the same to have a similar effect of the secondary currents.

GOVERNING EQUATIONS

Consider the open-channel flow at a high Reynolds number, and assume that the flow is uniform in the streamwise direction. If we denote the mean and fluctuating velocity components by $\overline{u_i}$ and u_i' in the *i*-direction, respectively, then the continuity equation and the momentum equations are given by

$$\frac{\partial \overline{u}_i}{\partial x_i} = 0 \tag{1}$$

$$\frac{\partial \overline{u}_i}{\partial t} + \overline{u}_j \frac{\partial \overline{u}_i}{\partial x_j} = -\frac{1}{\rho}\frac{\partial \overline{p}}{\partial x_i} + \frac{\partial}{\partial x_j}\left(\nu \frac{\partial \overline{u}_i}{\partial x_j}\right) - \frac{\partial \overline{u_i' u_j'}}{\partial x_j} - f_i + g_i \tag{2}$$

where ρ is the fluid density, $\overline{p}$ is the mean pressure, ν is the kinematic viscosity, $\overline{u_i' u_j'}$ denotes the Reynolds stress, g_i is the gravitational acceleration, and f_i is the *i*-component of the drag force due to vegetation given by

$$f_i = \frac{1}{2} C_D a \overline{u}_i \sqrt{\overline{u}^2 + \overline{v}^2 + \overline{w}^2} \tag{3}$$

where C_D is the drag coefficient and *a* is the vegetation density.

For a given flow field, the concentration of the passive scalar can be computed by solving the following Reynolds-averaged convection/diffusion equation:

$$\frac{\partial \overline{c}}{\partial t} + \overline{u}_i \frac{\partial \overline{c}}{\partial x_i} = \frac{\partial}{\partial x_i}\left(\lambda \frac{\partial \overline{c}}{\partial x_i} - \overline{u_i' c'}\right) \tag{4}$$

where $\overline{u_i' c'}$ is the scalar flux.

REYNOLDS STRESS MODEL FOR FLOW

The Reynolds stress in Eq.(2) is obtained by solving the transport equations of the Reynolds stress R_{ij} (= $\overline{u_i' u_j'}$) such as

$$\begin{aligned} \frac{\partial R_{ij}}{\partial t} + \overline{u}_k \frac{\partial R_{ij}}{\partial x_k} = & -\frac{\partial}{\partial x_k}\left(\overline{u_k' u_i' u_j'}\right) + \frac{1}{\rho}\left(\frac{\partial \overline{u_i' p'}}{\partial x_j} + \frac{\partial \overline{u_j' p'}}{\partial x_i}\right) - \left(R_{ik}\frac{\partial \overline{u}_j}{\partial x_k} + R_{jk}\frac{\partial \overline{u}_i}{\partial x_k}\right) \\ & - 2\nu \overline{\frac{\partial u_i'}{\partial x_l}\frac{\partial u_j'}{\partial x_l}} + \overline{\frac{p'}{\rho}\left(\frac{\partial u_j'}{\partial x_i} + p'\frac{\partial u_i'}{\partial x_j}\right)} \end{aligned} \tag{5}$$

On the right hand side of Eq.(5), the first and second terms are the transport of R_{ij} by diffusion, the third term is the production term by shear, the fourth term is the rate of dissipation of R_{ij}, and the fifth term is the transport of R_{ij} due to turbulent pressure-strain interactions. For open-channel flows, Choi and Kang (2001) carried out numerical experiments with various RSMs including three diffusion

models and five pressure-strain models. Choi and Kang found that the diffusion model of Mellor and Herring (1973) and the pressure-strain model of Speziale, Sarkar, and Gatski (1991) reproduce the measured data best. For the dissipation rate term, Choi and Kang used Rotta's (1951) model. In order to reflect the damping effect at the free surface, the combination of Shir's (1973) model and Gibson and Launder's (1978) model is added to the pressure-strain correlation term. With these sub models, Choi and Kang (2008) successfully simulated the mean flow and turbulence statistics of the open-channel and compound open-channel flows with vegetation.

ALGEBRAIC SCALAR FLUX MODEL FOR SOLUTE TRANSPORT

The scalar flux in Eq.(4) can be obtained with the help of the generalized gradient diffusion hypothesis by Daly and Harlow (1970) such as

$$\overline{u_i'c'} = -C_c \frac{k}{\varepsilon} \overline{u_i'u_k'} \frac{\partial \bar{c}}{\partial x_k} \tag{6}$$

where C_c is a model constant (= 0.18). The choice of GGDH model for modeling the scalar flux is based on numerical experiments reported by Kang and Choi (2008).

BOUNDARY CONDITIONS

Boundary conditions are required at the walls and at the free surface. It is assumed that the flow at the node closest to the wall obeys the standard logarithmic law. Since local equilibrium is assumed in the vicinity of the wall, the dissipation rate is set equal to the production of the turbulence kinetic energy. For the Reynolds normal stress at the wall, the zero gradient condition is used. For the Reynolds shear stress, the turbulent shear is set equal to the value from the logarithmic law. The free surface is treated as a symmetric plane for all dependent variables except for the dissipation rate of the turbulent kinetic energy (ε). For ε, the relationship by Naot and Rodi (1982) is prescribed in order to increase the dissipation level of turbulence kinetic energy at the free surface. Also, the boundary conditions for the solute concentration at the wall and the free surface are imposed to the zero-gradient condition.

SIMULATION RESULTS

The experimental conditions described in Yang (2009) are used in the numerical simulations. They are flow depth of 0.075m, channel width of 0.45, aspect ratio of 6, bottom slope of 0.0014, vegetation height of 0.035m, and vegetation density of 2.78 m^{-1}.

Figure 1 and Figure 2 show the contour of the streamwise mean velocity and secondary current vectors, respectively. Both simulated results and data measured by Yang (2009) are given for comparisons. Figure 1 shows that the velocity maximum occurs near the sidewall as well as near the center. Also, observed are isovels wavy in the lateral direction. In Figure 2, a large vortex rotating in the counter-clockwise direction is observed near the sidewall. This

vortex moves the high momentum fluids to the sidewall, resulting a maximum in the sidewall region. It can be seen that the numerical model successfully simulates the streamwise mean velocity and secondary currents.

In order to investigate the impact of submerged vegetation on the flow and solute transport, numerical experiments are carried out under smooth and rough bed conditions and with vegetation at densities of a = 0.1 m-1 and 0.5 m-1. Detailed conditions used in the computations are listed in Table 1. Since vegetation in the channel raises water level, bed slope and roughness height are varied to insure similar flow depth or Reynolds number. Due to this, the location of the injection points, aspect ratio (= 6.0), and depth ratio (= 2.14: flow depth to vegetation height ratio) are kept unchanged. The Reynolds number ranges between 38,600 – 44,200.

Figure 3 shows the simulated results of streamwise mean velocity. Comparing the smooth and rough bed flows reveals that the mean velocity near the sidewall is slightly larger for the rough bed flow, however, the difference is not significant. It is noteworthy that a velocity maximum near the sidewall is formed as the vegetation density increases. The velocity gradient in the lateral direction is observed to be milder for flows with vegetation compared with the smooth bed flow.

Figure 4 shows the secondary current vectors. For both smooth and rough bed flows, both free surface vortex and bottom vortex are seen. As the vegetation density increases, the bottom vortex, rotating in the counter-clockwise direction, is enlarged, occupying the whole depth near the sidewall for a = 0.5 m-1.

Figure 5(a) and 5(b) depict the distributions of the streamwise mean velocity and velocity gradient at y/B = 0.5, respectively. It can be seen in Figure 5(a) that submerged vegetation retards the flow over the entire depth compared with both smooth and rough bed flows. The submerged vegetation appears to induce velocity defect in the vegetation layer as the vegetation density increases. Figure 5(b) shows that the maximum velocity gradient occurs near the bed for both smooth and rough bed flows. However, for flows with submerged vegetation, a maximum of the velocity gradient is also observed near the vegetation height as well as near the bed. The higher velocity gradient induces higher rate of generation of the turbulent kinetic energy and thus Reynolds stress near the vegetation height. The high shear near the vegetation height will affect to increase the rate of the diffusion of the solute in the vertical direction.

Figure 6 shows the vertical distribution of the mean concentration with the streamwise distance. The mean concentrations are simulated results at y/B = 0.5. The dye is injected at a concentration of 250 ppb. The injection points are equally-spaced at x = 0 and z = h_p. The maximum concentration in the smooth bed flow is the largest. Then, the maximums in the rough bed flow and the vegetated flows follow. All profiles at x = 0.1 m seem to follow the Gaussian distribution. However, at x = 0.3 m, the mean concentration in the flow with vegetation at a = 0.5 m^{-1} becomes thicker near the bed, destroying the symmetry. Interestingly, for flows with vegetation, the mean concentration near the vegetation height decreases quickly, but the concentration near the bed increases fast. This indicates that the solute is diffused over the depth faster in the vegetated flow. That is, in the flow with submerged vegetation, the advection in the streamwise direction is less

fast due to retarded velocity, but the diffusion in the vertical direction takes place faster due to strengthened shear near the vegetation height.

The distribution of the mean concentration at x = 0.3 m is given in Figure 7. For the smooth bed flow, the mean concentration takes a circular distribution with the maximum at the centers of the injection points. Contrastingly, for the vegetated flow at a = 0.5 m^{-1}, the dye is diffused over the depth and width, making the distribution uniform, except for the region close to the sidewall. This is because the velocity gradient in the vertical direction near the sidewall is smaller than that near the center.

Figure 8 shows the same plots at x = 1.5 m. It can be seen that the distribution of the mean concentration is nearly two-dimensional except for the sidewall region for both smooth and rough bed flows. For the flow with vegetation, the impact of submerged vegetation is clearly seen. That is, in Figure 8(d), the counter-clockwise rotating vortex moves the dye to the lower-left corner, making the maximum concentration there and bulges the contour towards the direction of the secondary flows.

Figure 9 shows the lateral distribution of turbulent Schmidt number (σ_{tz}) for the smooth bed flow and the vegetated flow of a = 0.5 m^{-1}. The turbulent Schmidt number, averaged over the depth, is defined by the ratio of eddy viscosity to eddy diffusivity. The average values of σ_{tz} are 1.04 and 0.83 for the smooth bed flow and vegetated flow, respectively. This indicates the rate of diffusion of the scalar flux is greater than that of the momentum in the flow with submerged vegetation, while they are about the same in the smooth bed flow.

CONCLUSIONS

A numerical model for the prediction of the solute transport in the depth-limited open-channel flow with submerged vegetation is proposed. The algebraic scalar flux model by Daly and Harlow (1970) is used to solve the transport equation. For the flow, the Reynolds stress model by Choi and Kang (2008) is employed.

The model is applied to Yang's (2009) experiment, successfully reproducing the flow concentration in the sidewall region. That is, a velocity maximum occurs near the sidewall region as well as near the center. This happens because the counter-rotating vortex moves high momentum fluids from the center to the sidewall region, which is supported by both measured data and simulated results of the secondary current vectors.

Then, the model is applied to various cases of solute transports, namely solute transports in the smooth bed flow, in the rough bed flow, and in the flows with submerged vegetation. The Reynolds numbers of the flows are made similar to investigate the impact of submerged vegetation on the solute transport. It is observed that, for the vegetated flow, the bottom vortex, rotating in the counter clockwise direction, becomes dominant in the sidewall region, while both the free surface vortex and bottom vortex are observed in the flow without vegetation. It is found that the solute is diffused faster near the vegetation height for the vegetated flow compared with the flow without vegetation. This resulted in a turbulent Schmidt number of 0.83 for the flow vegetated at a = 0.5 m^{-1}, indicating that the rate of diffusing the solute is greater than that of the momentum. For the smooth

bed flow, a turbulent Schmidt number close to unity is obtained.

ACKNOWLEDGEMENTS
This research was supported by a grant (06B01) from the Technical Innovation of Construction Program funded by Ministry of Land, Transport, and Maritime Affairs of Korea government.

REFERENCES

Ackerman, J.D. and Okubo, A. (1993). "Reduced mixing in a marine macrophyte canopy." *Functional Ecology*, 7, 305-309.

Choi, S.-U. and Kang, H. (2001). "Numerical tests of Reynolds stress models in the computations of open-channel flows." *Proceedings of 8-th Flow Modeling and Turbulence Measurements*, Tokyo, Japan.

Choi, S.-U. and Kang, H. (2004). "Reynolds stress modeling of vegetated open-channel flows." *Journal of Hydraulic Research*, IAHR, 42(1), 3-11.

Daly, B.J. and Harlow, F.H. (1970). "Transport equations in turbulence." *Physics of Fluids*, 13, 2634-2649.

Ghisalberti, M. and Nepf, H.M. (2002). "Mixing layers and coherent structures in vegetated aquatic flows." *Journal of Geophysical Research*, AGU, 107(C2), 3-1-3-11.

Gibson, M.M. and Launder, B.E. (1978). "Ground effects on pressure fluctuations in the atmospheric boundary layer." *Journal of Fluid Mechanics*, 86, 491-511.

Ikeda, S. and Kanazawa, M. (1996). "Three dimensional organized vortices above flexible water plants." *Journal of Hydraulic Engineering*, ASCE, Vol. 122, No. 11, pp. 634-640.

Kang, H. and Choi, S.-U. (2008). "Scalar Flux Modeling of Solute Transport in Open-Channel Flows: Numerical Tests and Effects of Secondary Currents." *Journal of Hydraulic Research*, IAHR, submitted.

Lopez, F. and Garcia, M. (2001). "Mean flow and turbulence structure of open-channel flow through non-emergent vegetation." *Journal of Hydraulic Engineering*, ASCE, 127(5), 392-402.

Mellor, G.L. and Herring, H.J. (1973). "A survey of mean turbulent field closure." *AIAA Journal*, 11, 590-599.

Naot, D. and Rodi, W. (1982). "Calculation of secondary currents in channel flows." *Journal of the Hydraulics Division*, ASCE, 108(HY8), 948-968.

Nezu, I. and Onitsuka, K. (2001). "Turbulent structures in partly vegetated open-channel flows with LDA and PIV measurements." *Journal of Hydraulic Research*, IAHR, 39(6), 629-642.

Rotta, J.C. (1951). "Statistische theorie nichthomogener turbulenz." *Zeitschrift fur Physik*, 129, 547-572.

Shimizu, Y. and Tsujimoto, T. (1994). "Numerical analysis of turbulent open-channel flow over a vegetation layer using a k-ε turbulence model." *Journal of Hydroscience and Hydraulic Engineering*, JSCE, 11(2), 57-67.

Shir, C.C. (1973). "A preliminary study of atmospheric turbulent flow in the idealized planetary boundary layer." *Journal of Atmospheric Science*, 30, 1327.

Speziale, C.G., Sarkar, S., and Gatski, T. (1991). "Modeling the pressure strain correlation of turbulence: an invariant dynamical systems approach." *Journal*

of Fluid Mechanics, 227, 245-272.

Xiaohui, S. and Li, C.W. (2002). "Large eddy simulation of free surface turbulent flow in partly vegetated open-channels." *International Journal for Numerical Methods in Fluids*, 39, 919-937.

Yang, W. (2008). Experimental study of turbulent open-channel flows with submerged vegetation, Ph.D. Thesis, Yonsei University, Korea.

Table 1. Conditions used in Numerical Computations

case	Depth H(m)	Width B(m)	Aspect ratio	Slope (×10-3)	Veg. density a (m^{-1})	Veg. Height h_p (m)	Roughness Height (m)	Mean velocity (m/s)	Reynolds number
S1	0.075	0.45	6.0	1.793	-	-	-	0.785	44,164
R1				2.69	-	-	0.002	0.776	43,657
V5				2.69	0.1	0.035	-	0.718	40,394
V5				6.05	0.5	0.035	-	0.687	38,650

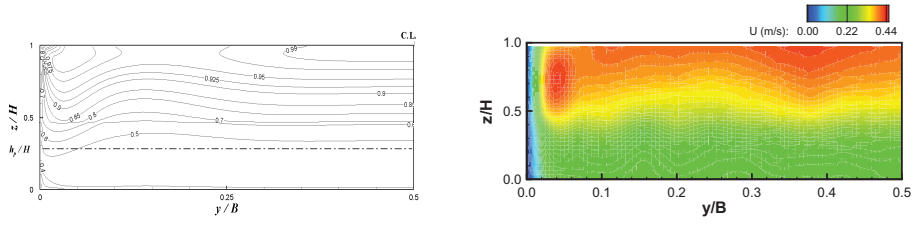

(a) computed (b) measured by Yang (2009)

Figure 1. Streamwise mean velocity

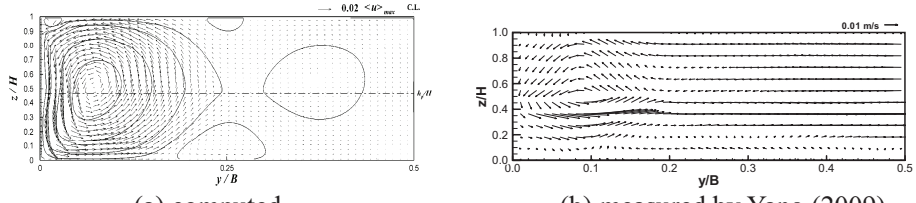

(a) computed (b) measured by Yang (2009)

Figure 2. Secondary current vectors

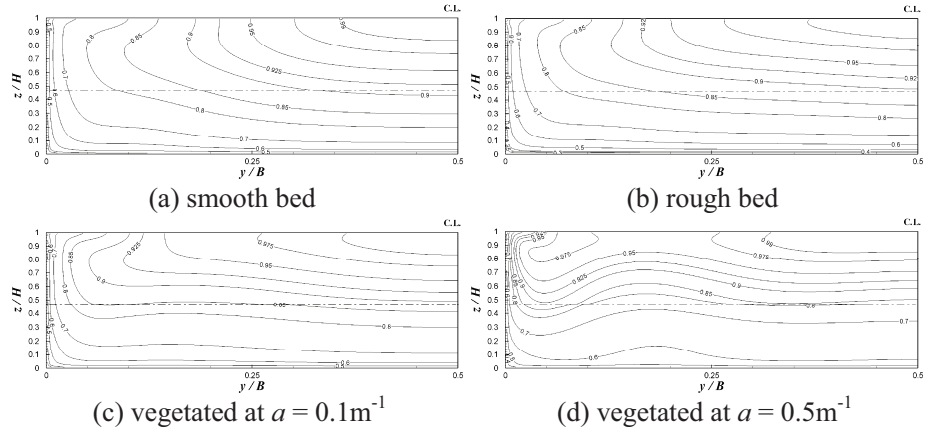

(a) smooth bed (b) rough bed

(c) vegetated at $a = 0.1m^{-1}$ (d) vegetated at $a = 0.5m^{-1}$

Figure 3. Streamwise mean velocity

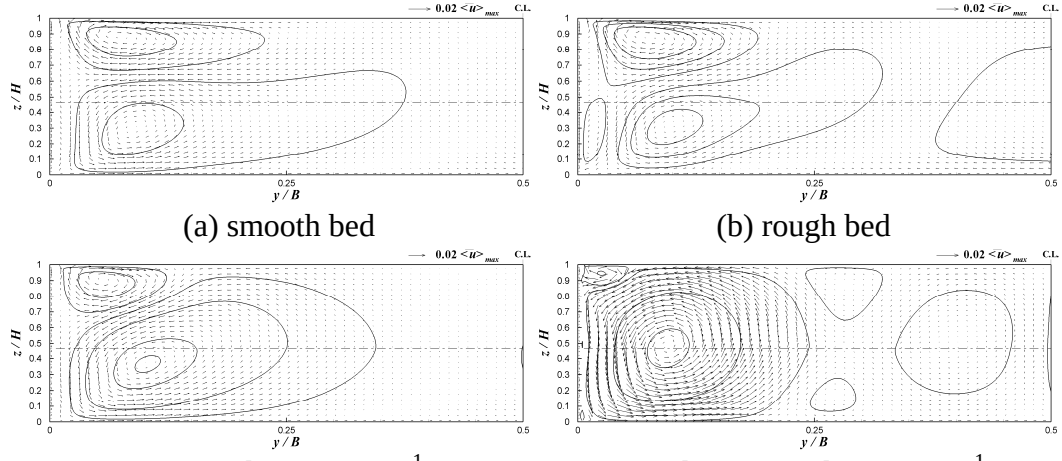

(a) smooth bed (b) rough bed

(c) vegetated at a = 0.1m^{-1} (d) vegetated at a=0.5m^{-1}

Figure 4. Secondary current vectors

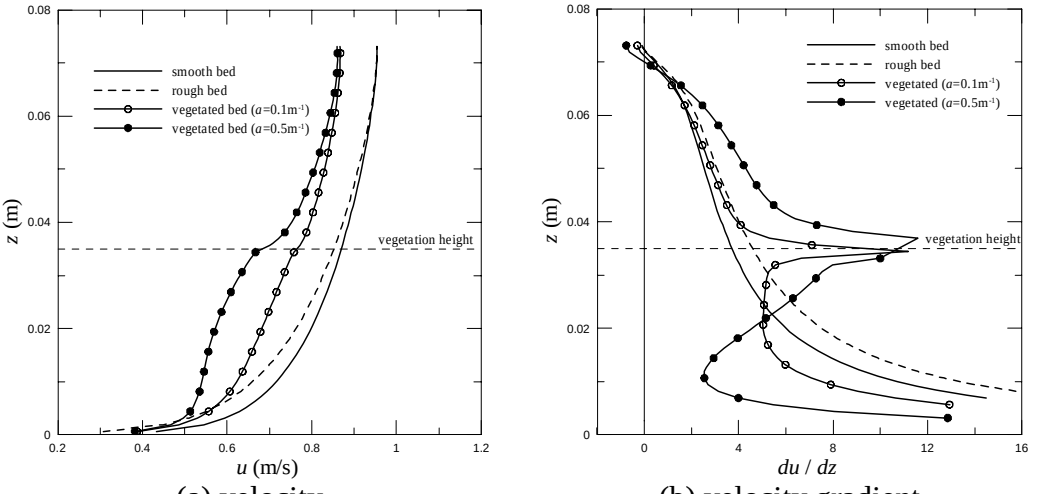

(a) velocity (b) velocity gradient

Figure 5. Vertical distributions of streamwise mean velocity and velocity gradient at $y = 0.5B$

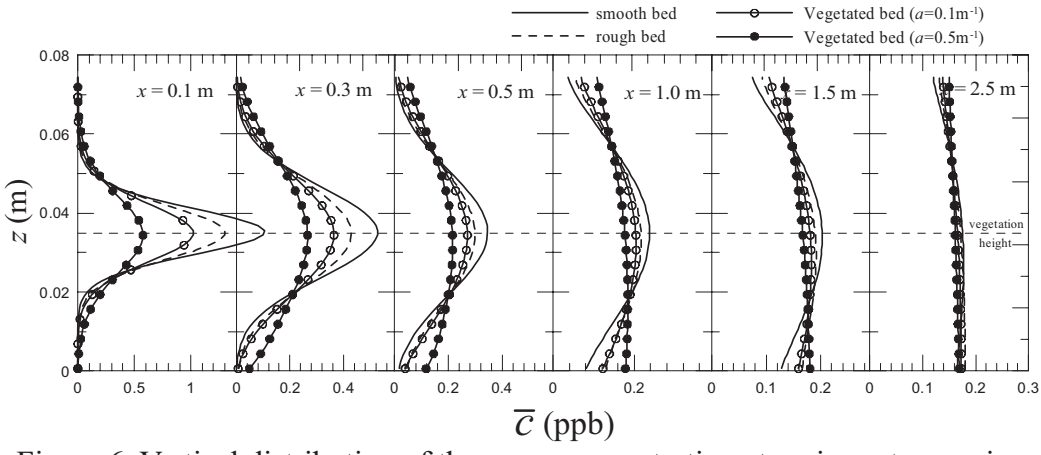

Figure 6. Vertical distribution of the mean concentration at various streamwise locations (at $y = 0.5B$)

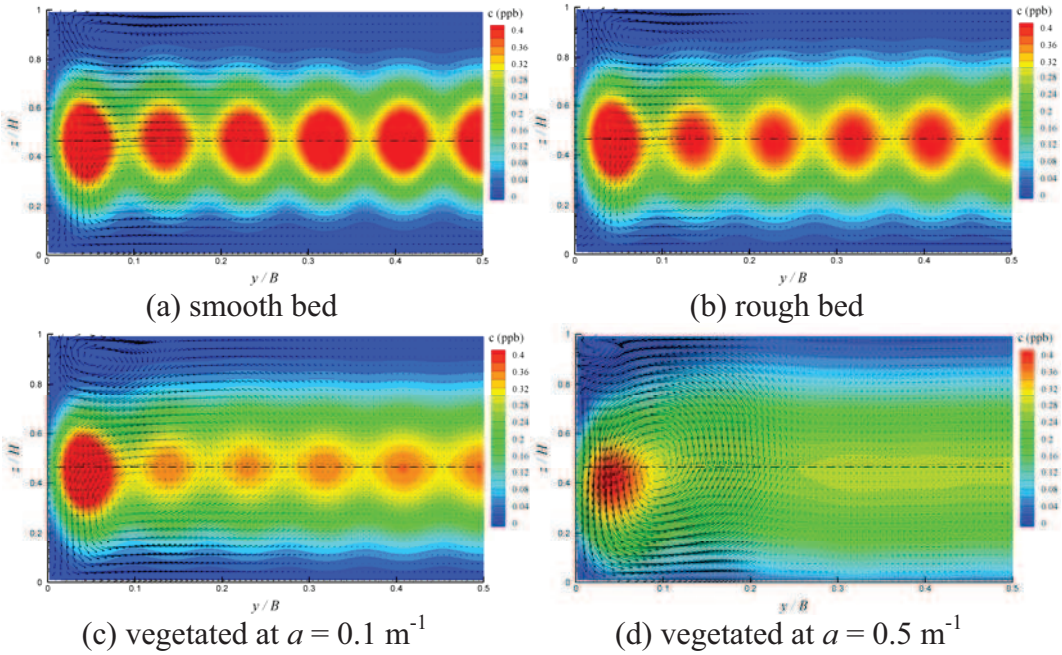

(a) smooth bed (b) rough bed

(c) vegetated at $a = 0.1$ m^{-1} (d) vegetated at $a = 0.5$ m^{-1}

Figure 7. Mean concentration contours at $x = 0.3$ m

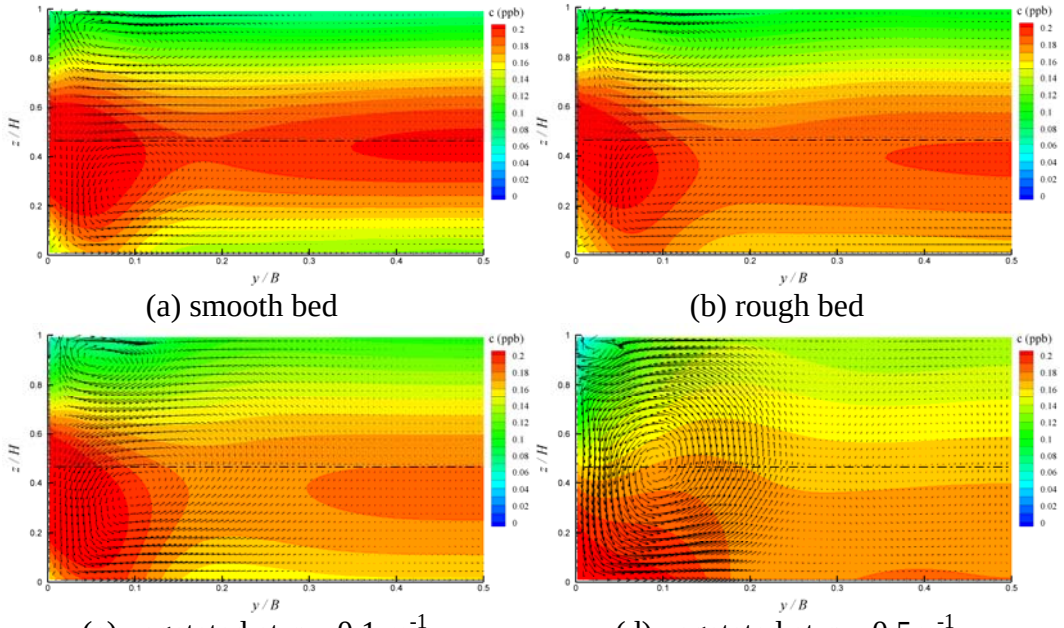

(a) smooth bed (b) rough bed

(c) vegetated at a = 0.1 m^{-1} (d) vegetated at a = 0.5m^{-1}

Figure 8. Mean concentration contours at x = 1.5 m